An Optimized Efficiency-Based Control Strategy for Islanded Paralleled PV Micro-Converters*

Han-Dong Gui[1], *Student Member, IEEE*, Yue Zhang[1],
Zhiliang Zhang[1], *Senior Member, IEEE*, and Yan-Fei Liu[2], *Fellow, IEEE*

[1]Jiangsu Key Laboratory of New Energy Generation and Power Conversion
Nanjing University of Aeronautics andAstronautics, Nanjing, Jiangsu, P. R. China
[2]Department of Electrical and Computer Engineering
Queen's University, Kingston, Ontario, Canada, K7L 3N6
ghdcat@nuaa.edu.cn, yuezhang@nuaa.edu.cn, zlzhang@nuaa.edu.cn and yanfei.liu@queensu.ca

***Abstract*— This paper analyzes the operation of PV modules in islanded paralleled PV applications under different solar irradiance condition in detail. When the batteries in the system are fully charged, the PV panels only need to generate power depending on the load and may not necessarily track the maximum power point (MPP), which exists extensively. In order to optimize the system efficiency in this situation, an efficiency-based model is built and a control strategy that can distribute the output power of different PV modules to find minimum total loss of the system is proposed. The system efficiency can be optimized adaptively under different load and irradiance condition with the proposed strategy. A distributed system prototype with three converters in parallel has been built and tested. The experimental results verified the benefits of the proposed strategy.**

***Keywords*---- islanded paralleled PV applications; micro-converter; system efficiency; power distribution.**

I. INTRODUCTION

The applications of distributed photovoltaic (PV) generation systems based on micro-converters are increasing rapidly nowadays. In such systems, modules with PV panels and high step-up converters are connected in parallel to offer power to a high voltage DC bus and energy storage units like batteries and super capacitors are also required.

The intended operation of the PV system can be divided into two operating conditions: grid-connected system and islanded system [1]. In the grid-connected systems, the DC bus is connected to a centralized inverter which supports the main grid. In this configuration, the system can exchange power with the main grid and all PV modules work at maximum power point (MPP). The islanded systems are widely applied in remote places where no main grid is available or the quality of the power grid is not guaranteed, such as the mountain areas, islands or even space stations. Fig. 1 shows the structure of a typical islanded distributed PV system. Compared to the conventional centralized, string and multi-string structure, the paralleled micro-converters own several advantages such as higher MPPT efficiency, more flexibility in the system expansion, less installation and manufacturing cost in mass production.

*This work is supported by the Priority Academic Program Development of Jiangsu Higher Education Institutions and the Lite-On Research Funding.

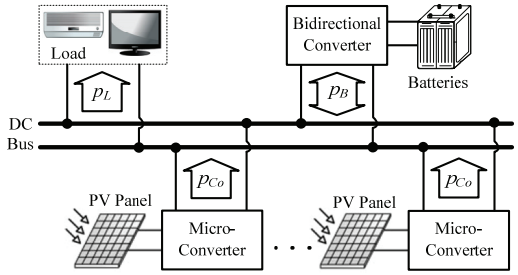

Fig. 1 Structure of an islanded distributed PV system

Much effort has been paid to the current share of different modules in paralleled applications [2]-[5]. However, these researches mainly focus on improving the stable and dynamic performance and most assumption is that load is equally distributed in different modules. However, the loss of single converter varies when its load changes, so different load distribution can cause different total loss of the system. Hence the total loss of equal distribution is not necessarily to be minimum and the system efficiency is not optimal. Phase shedding can improve the system efficiency for the multi-phase converters [6], an improved control scheme without the communication signals is analyzed in [7], an accurate parameter analysis to minimize loss is proposed in [8] and game theoretic approach is applied in [9]. However, these control techniques are not suitable for PV applications with wide input voltage range due to irradiance condition, so it is desired that a control strategy can adjust adaptively to find the minimum total loss and optimize the system efficiency when irradiance condition changes.

In order to solve the problems, a control strategy for islanded paralleled PV applications is proposed to optimize the system efficiency of the system in this paper.

II. OPERATION OF PV MODULES UNDER DIFFERENT SOLAR IRRADIANCE CONDITION

The characteristic equation for the PV model is given by

$$I = I_{LG} - I_{os}\{\exp[\frac{q}{AkT}(V + IR_s)] - 1\} - \frac{V + IR_s}{R_{sh}} \quad (1)$$

$$I_{LG} = [I_{SCR} + K_I(T - 25)] \cdot E / 100 \quad (2)$$

where I and V are the output current and voltage of PV panels, I_{LG} is the light-generated current, I_{os} is the reverse

saturation current, A=1.92 is the ideality factors, K is Boltzmann's constant, q is the electronic charge, R_s is the series resistance, R_{sh} is the shunt resistance, I_{SCR} is the short-circuit current at 25 °C and 1000 W/m^2, K_I=0.0017 A/°C is the short circuit current temperature coefficient at I_{SCR}, T is the PV cell temperature, E is the solar irradiance in W/m^2.

It can be seen from (1) and (2) that the output power is approximately proportional to solar irradiation E [10].

The average irradiance per day varies in different seasons. Table I shows the average solar irradiance per day of Lhasa in Tibet, China in different months, 2002. It is observed that the lowest irradiance in December is much less than the highest in June so the ability for the PV panels to power the load is weakest in December and strongest in June.

Table I Average solar irradiance per day in different months in Lhasa

Month	1	2	3	4	5	6
Irradiance (MJ/m^2)	15.82	18.00	20.32	22.22	24.68	**26.19**
Month	7	8	9	10	11	12
Irradiance (MJ/m^2)	22.20	22.29	20.80	19.99	17.11	**14.96**

In order to guarantee that the system can operate normally in all months, the rated output power of the PV panels should be designed to supply the load in the worst irradiance month. As a result, in the months with the abundant solar irradiance, the maximum output power of the PV panels is highly possible to be more than the demand of the load.

In the period of one day, the solar irradiance can be simulated as a sinusoidal function [11]. Fig. 2 illustrates the operation of a PV system as shown in Fig. 1 in 24 hours based on the data in Lhasa above. Assuming that the load is constant as 167W and the output power of the PV panels is the sinusoidal line and the maximum output power is 1000W. Region I and Region II are the energy supplied to the load by the batteries and the PV panels respectively. Region III is the energy that the PV panels charge the batteries. The shaded area of Region III should be equal to that of Region I since the discharged energy and charged energy into the batteries has to be equal.

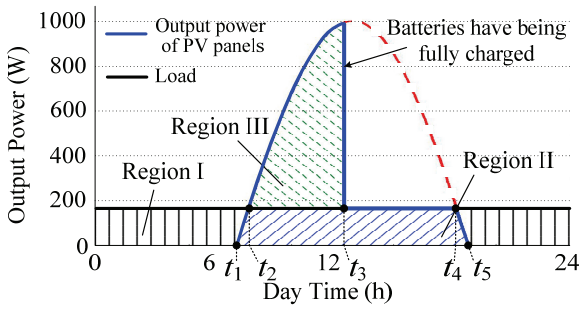

Fig. 2 Operation condition of the PV panels in one day

Before t_1 and after t_5, the PV panels cannot produce power and the load is fed by the batteries. From t_1 to t_2 and t_4 to t_5, maximum output power of the PV panels is less than the demand of the load, so the PV panels and the batteries provide the power to the load together. From t_2 to t_3, maximum output power of the PV panels exceeds the demand of the load, so the PV panels feed the load and charge the batteries at the same time. At t_3, the batteries have been fully charged, so from t_3 to t_4, the PV panels only need to generate power depending on the load which is 167W though they have the ability to export more power as the red dotted line.

In Fig. 3, Part A is the total output time of the PV panels (t_1 to t_5 in Fig. 2) and Part B is the time that PV panels do not need to track MPP (t_3 to t_4 in Fig. 2) per day in different months. It can be seen that in June, Part A is 10.16h while Part B is 5.45h. Except December, Part B exists in every month. During a year, Part B makes up 38% of Part A. So the operating condition where the PV panels do not need to track MPP exists widely in such islanded PV applications. Therefore, it is beneficial to optimize the system efficiency in this situation.

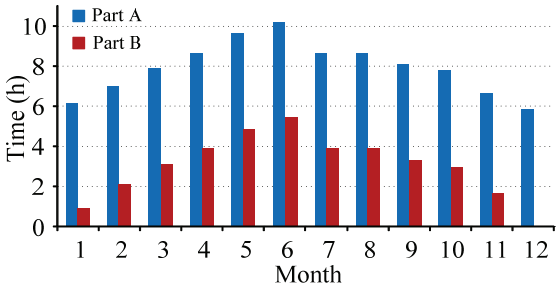

Fig. 3 Time of the PV panels without tracking MPP per day in different months

III. Proposed Efficiency Model and Control Strategy

A. Proposed Efficiency Model under Different Load and Irradiance Condition

Table II Nomenclature

p_{Co}	Output power of single converter	η_C	Efficiency of single converter
p_o	Total output power	p_{Cin}	Input power of single converter
p_{PV}	Output power of PV panels	p_{in}	Total input power
v_{Cin}	Input voltage of single converter	v_{PV}	Output voltage of PV panels
η	System efficiency	i_{Cin}	Input current of single converter
i_{PV}	Output current of PV panels	E	Solar irradiance

The efficiency curve of the individual converters can be fitted as a function of p_{Co} and v_{Cin}

$$\eta_C = \frac{p_{Co}}{p_{Cin}} = f(p_{Co}, v_{Cin}) \tag{3}$$

p_{Cin} is equal to p_{PV} and is directly related to E. So p_{Cin} can be expressed as a function of v_{Cin} and E

$$p_{Cin} = p_{PV} = i_{PV} \cdot v_{PV} = i_{Cin} \cdot v_{Cin} = g(v_{Cin}, E) \tag{4}$$

E is hard to measure, since for a PV panel, there is a one-to-one correspondence between E and the combination of v_{Cin} and i_{Cin}, combining (3) with (4) to eliminate E, the function of the efficiency curve can be expressed as

$$\eta_C = h(f, g) = h(p_{Co}, E) = h(p_{Co}, v_{Cin}, i_{Cin}) \tag{5}$$

In a system consisting of n PV modules, the system efficiency η can be expressed by

$$\eta=\frac{p_o}{p_{in}}=\frac{p_o}{\sum_{i=1}^{n}p_{Cin\_i}}=\frac{p_o}{\sum_{i=1}^{n}\frac{p_{Co\_i}}{\eta_{C\_i}}}=\frac{p_o}{\sum_{i=1}^{n}\frac{p_{Co\_i}}{h(p_{Co\_i},v_{Cin\_i},i_{Cin\_i})}} \quad (6)$$

When the demand of the load is certain, the maximum efficiency means the minimum loss and input power. So the aim of the control strategy is to distribute the load and find the point of minimum input power P_{in_min}.

B. Control Structure and Proposed Control Strategy

Fig. 4 shows the control structure and the master-slave mode is used. The PV panels and the converters are the slave units that are connected in parallel to the DC bus. The total output power P_o is examined and transferred to master control unit. The master unit calculates the distributed current according to P_o and v_{Cin}, i_{Cin} of each PV panel and sends the reference p_{Co_r} to each converter to realize the distribution.

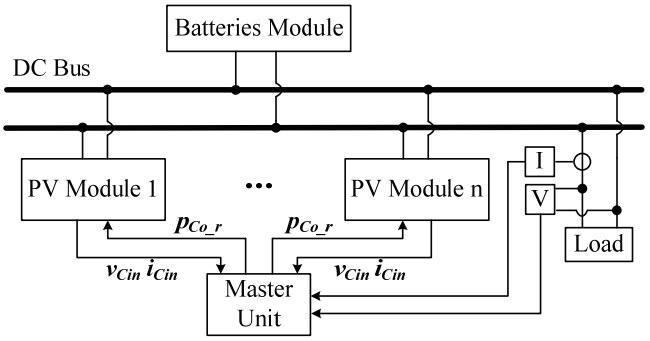

Fig. 4 Control structure

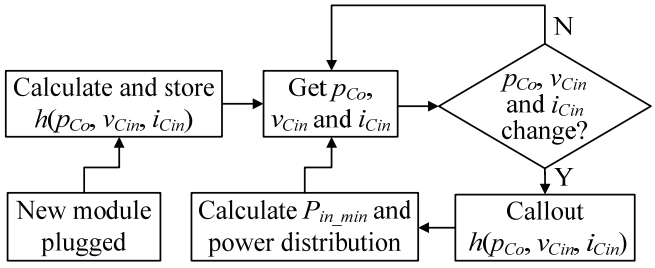

Fig. 5 Diagram of proposed control strategy

Fig. 5 shows the diagram of the proposed control strategy. When an additional PV module is plugged into, the master unit initially calculates the functions of h (p_{Co}, v_{Cin}, i_{Cin}) according to the data integrated in the PV module. Each combination of v_{Cin} and i_{Cin} corresponds to a unique irradiance condition. Then the master unit saves these functions into its storage preparing for calculating the load distribution. After the system starts operating, the master unit obtains information of P_o, v_{Cin} and i_{Cin} from the load and each module in real time. Then the master unit callouts the corresponding h (p_{Co}, v_{Cin}, i_{Cin}) of each module from the storage and calculates the minimum input power P_{in_min} by Lagrange multiplier method according to (4) and get the output power distribution. The converters operate according to the distribution reference p_{Co_r} given by the master unit. When P_o or v_{Cin}, i_{Cin} changes, the master unit re-callouts the functions and calculate the optimal load distribution again. So the proposed strategy can keep the system operating at highest efficiency point to a greatest extent when the load and irradiance condition changes.

C. Description of the Converter Applied in the Strategy

The high voltage-gain LLC converter proposed in [12] is used. Fig. 6 and Fig. 7 illustrate the main circuit and the tested efficiency of the converter respectively.

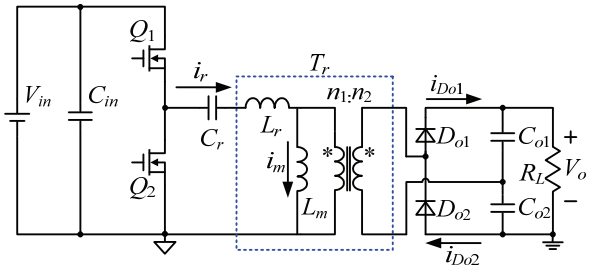

Fig. 6 Main circuit of high voltage-gain LLC converter

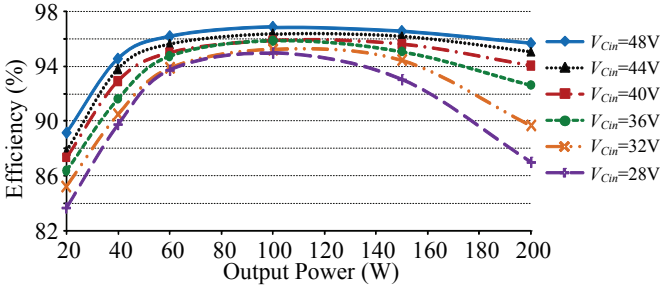

Fig. 7 Efficiency of the converter under different input voltages

Fig. 8 shows the curves of function h under different solar irradiance. It can be seen that different irradiance results in different curves.

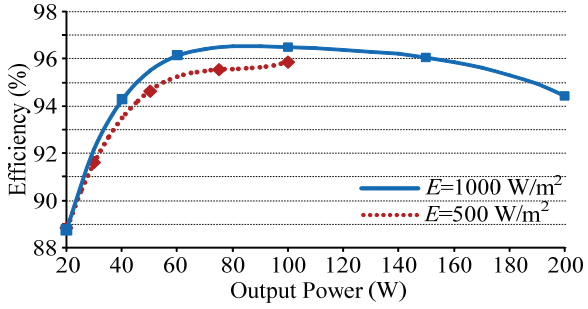

Fig. 8 Curves of h under different irradiance

D. Simulation Results and Discussion

A simulation system model is established in Matlab. In the system, three 200W converters in [12] operate in parallel and the control strategy above is applied. Fig. 9 to Fig. 11 illustrate the load distribution among three converters and comparison of system efficiency between proposed control strategy and equal distribution method under different irradiance, where E_i (i=1, 2, 3) represents the solar irradiance on each PV panel.

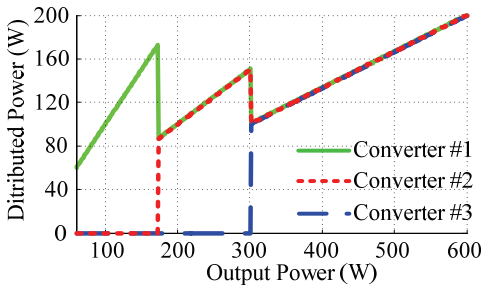

(a) Load distribution among three converters

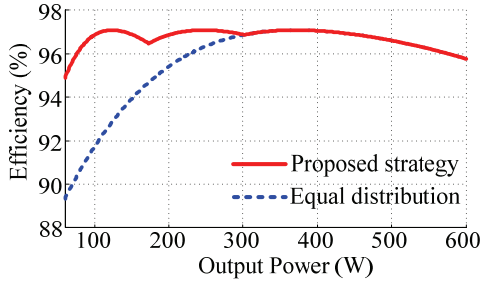

(b) Comparison of system efficiency

Fig. 9 Load distribution and comparison of system efficiency when E_1= E_2= E_3=1000 W/m^2

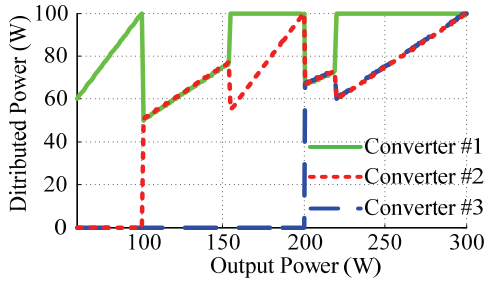

(a) Load distribution among three converters

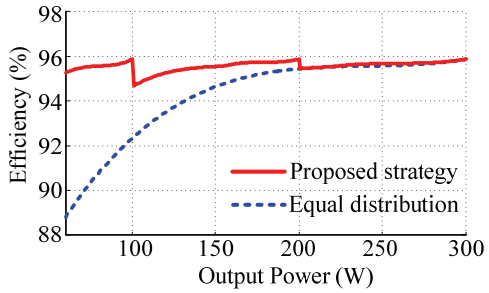

(b) Comparison of system efficiency

Fig. 10 Load distribution and comparison of system efficiency when E_1= E_2= E_3=500 W/m^2

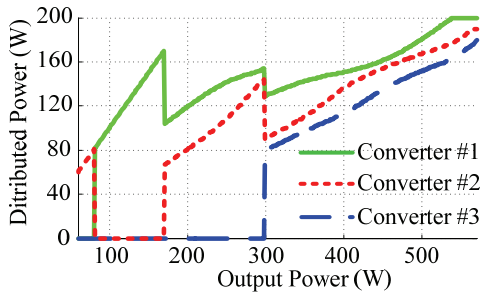

(a) Load distribution among three converters

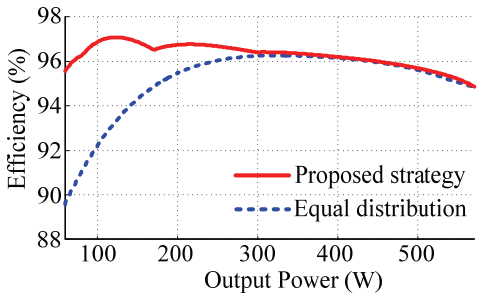

(b) Comparison of system efficiency

Fig. 11 Load distribution and comparison of system efficiency when E_1=1000 W/m^2, E_2=950 W/m^2, E_3=900 W/m^2

Table III lists the load distribution which corresponds to Fig. 10 (a). There are five periods and the load distribution in each period is calculated by the control strategy.

Table III Load distribution of three converters when E_1= E_2= E_3=500 W/m^2

P_o (W)	Load of #1 (W)	Load of #2 (W)	Load of #3 (W)
60–100	P_o	0	0
101–154	P_o/2	P_o/2	0
155–200	100	P_o-100	0
201–218	P_o/3	P_o/3	P_o/3
219–300	100	(P_o-100)/2	(P_o-100)/2

In Fig. 9 (a) and Fig. 11 (a), when the irradiance from 1000 W/m^2 changes to 950 W/m^2 and 900 W/m^2, there is a great difference in load distribution. From Fig. 9 (b) to Fig. 11 (b), the system efficiency is improved significantly especially under light load.

E. Application Extension

The proposed strategy can also extend to general paralleled applications. When the paralleled converters with different topologies and power ratings are operating, the strategy can be applied. Besides the 200 W high voltage-gain LLC converter in [12], another two converters in [13] and [14] are applied and their power rating is 250W and 100W. Fig. 12 shows the efficiency curve of the converters.

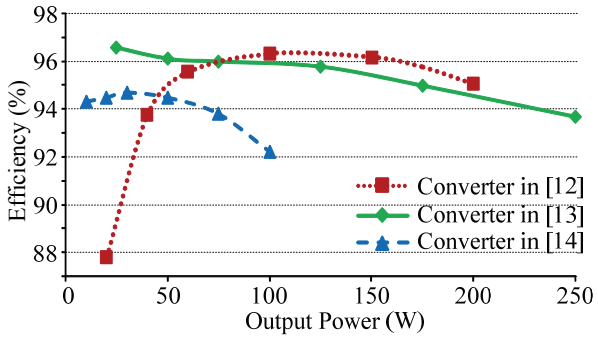

Fig. 12 Efficiency of three converters

Fig. 13 illustrates the load distribution among three converters and Fig. 14 illustrates the comparison of system efficiency between proposed control strategy and equal distribution method. It is noted that the strategy improves the system efficiency significantly.

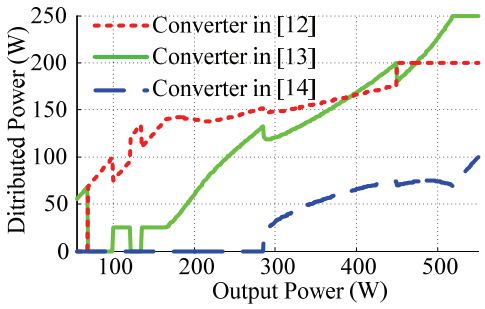

Fig. 13 Load distribution among three converters

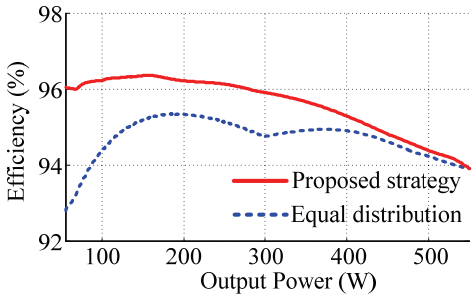

Fig. 14 Comparison of system efficiency

IV. Experimental Results and Discussion

To verify the functionality of the proposed strategy, a distributed system has been built. The system consists of three paralleled 200W high voltage-gain LLC converters proposed in [12] and applied the proposed control structure and strategy. The photo of the system is illustrated in Fig. 15. The irradiance of the three converters is 1000 W/m^2, 950 W/m^2 and 900 W/m^2 respectively.

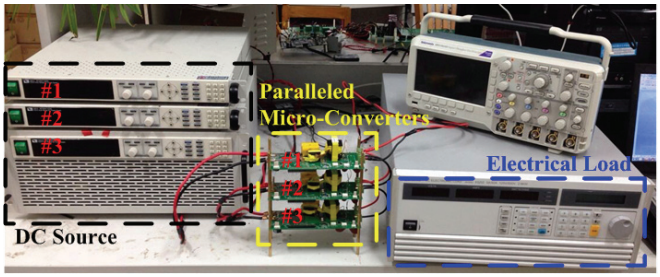

Fig. 15 Photo of the system

Fig. 16 highlights ZVS and ZCS of the LLC converter for high efficiency.

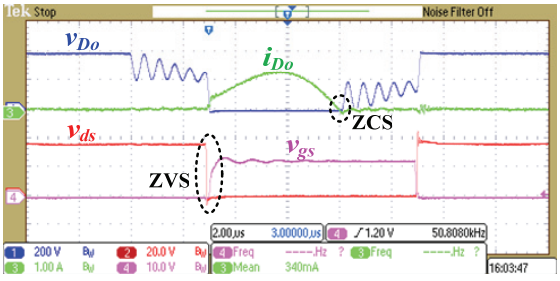

Fig. 16 ZVS and ZCS of the converter

Fig. 17 illustrates the load distribution that agrees with the simulation result of Fig. 11 (a). When the load is 300 W, the load distribution of three converters is 130 W, 90W and 80W respectively, and the magnitude of current through the output diodes of the three converters in Fig. 18 can verify the load distribution. When the load is 200 W, the irradiance of the module is 900 W/m^2 is cut off and the load distribution of the rest two modules is 120 W and 80 W. When the load is 100 W, only the module with irradiance of 1000 W/m^2 is operating. The load distribution can also be observed from Fig. 19 and Fig. 20.

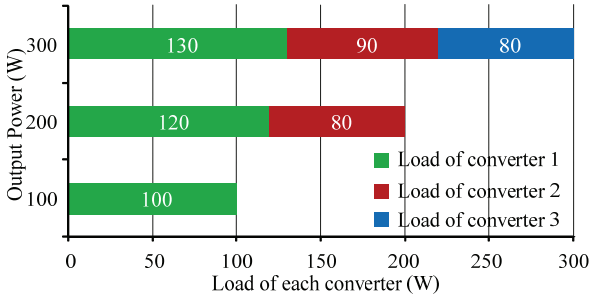

Fig. 17 Load distribution among three converters

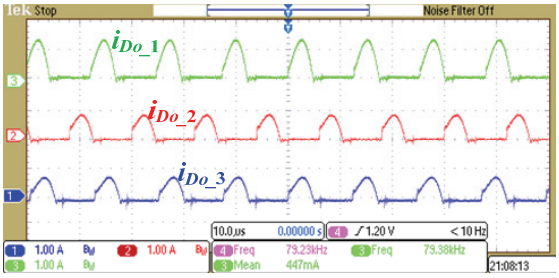

Fig. 18 Current through output diodes when P_o is 300 W

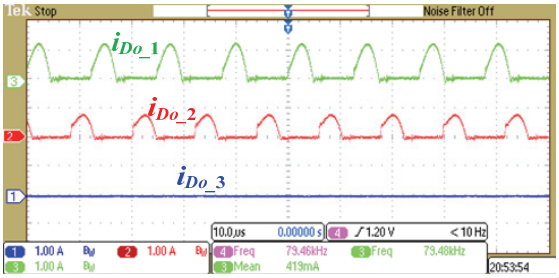

Fig. 19 Current through output diodes when P_o is 200 W

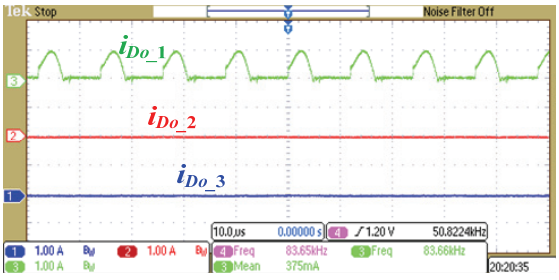

Fig. 20 Current through output diodes when P_o is 100 W

Fig. 21 shows the comparison between tested system efficiency with the proposed strategy and equal distribution

method under different irradiance. It is observed that the strategy can improve the system efficiency significantly. The improvement is 6.1% and 6.4% when the irradiance is 1000 W/m^2 and 500 W/m^2 respectively.

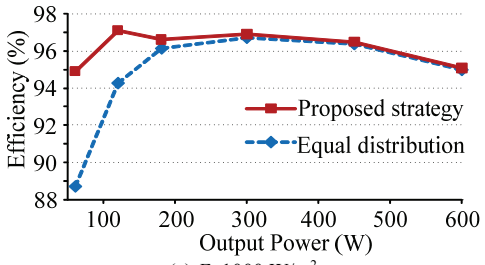

(a) E=1000 W/m^2

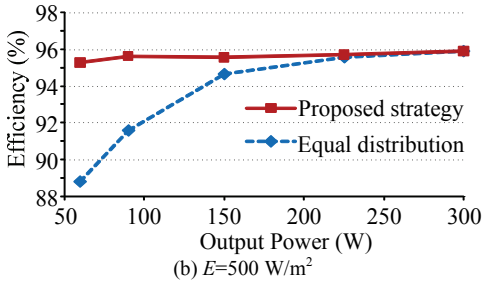

(b) E=500 W/m^2

Fig. 21 Comparison between tested system efficiency with the proposed strategy and equal distribution method

V. Conclusion

In this paper, the operation of the PV modules in islanded paralleled PV applications is analyzed in detail and the result shows that with the irradiance condition changing, the situation exists extensively in which the PV panels do not need to operate at MPP. In order to optimize the system efficiency in this situation, an optimized efficiency-based model is built and a control strategy to distribute the load of different PV modules is proposed. With the strategy, the system efficiency can be optimized adaptively under different load and irradiance condition and the strategy can be extended to more general application cases. Compared to the traditional equal distribution control, the efficiency improvement with the proposed control is 6.1% and 6.4% when the irradiance is 1000 W/m^2 and 500 W/m^2 respectively.

References

[1] T. L. Vandoorn, C. M. Ionescu, J. D. M. De Kooning, R. De Keyser and L. Vandevelde, "Theoretical analysis and experimental validation of single-phase direct versus cascade voltage control in islanded microgrids," *IEEE Trans. Ind. Electron.*, vol. 60, no. 2, pp. 789–798, Feb. 2013.

[2] N. Hur and K. Nam, "A robust load-sharing control scheme for parallel-connected multisystems," *IEEE Trans. Ind. Electron.*, vol. 47, no. 4, pp. 871–879, Aug. 2000.

[3] J. He and Y. W. Li, "An enhanced microgrid load demand sharing strategy," *IEEE Trans. Power Electron.*, vol. 27, no. 9, pp. 3984–3995, Sep. 2012.

[4] A. G. Beccuti, M. Kvasnica, G. Papafotiou, and M. Morari, "A decentralized explicit predictive control paradigm for parallelized DC-DC circuits," *IEEE Trans. Power Electron.*, vol. 21, no. 1, pp. 136–148, Jan. 2013.

[5] S. Anand, B. G. Fernandes and J. M. Guerrero, "Distributed control to ensure proportional load sharing and improve voltage regulation in low-voltage DC microgrids," *IEEE Trans. Power Electron.*, vol. 28, no. 4, pp. 1900-1913, Apr. 2013.

[6] J. T. Su and C. W. Liu "A novel phase-shedding control scheme for improved light load efficiency of multiphase interleaved DC–DC converters," *IEEE Trans. Power Electron.*, vol. 28, no. 10, pp. 4742-4752, Oct. 2013.

[7] S. Effler, M. Halton and K. Rinne, "Efficiency-based current distribution scheme for scalable digital power converters," *IEEE Trans. Power Electron.*, vol. 26, no. 4, pp. 1261-1269, Apr. 2011.

[8] H. Renaudineau, A. Houari, A. Shahin, J. P. Martin, S. Pierfederici, F. Meibody-Tabar and B. Gerardin, "Efficiency optimization through current-sharing for paralleled DC–DC boost converters with parameter estimation," *IEEE Trans. Power Electron.*, vol. 29, no. 2, pp. 759-767, Feb. 2014.

[9] P. Bartal and I. Nagy, "Game theoretic approach for achieving optimum overall efficiency in DC/DC converters," *IEEE Trans. Ind. Electron.*, vol. 61, no. 7, pp. 3202–3209, Jul. 2014.

[10] E. Koutroulis, K. Kalaitzakis and N. C. Voulgaris, "Development of a microcontroller-based, photovoltaic maximum power point tracking control system," *IEEE Trans. Power Electron.*, vol. 16, no. 1, pp. 46-54, Jan. 2001.

[11] G. M. Tina, C. Ventura and S. D. Fiore, "Sub-hourly irradiance models on the plane of array for photovoltaic energy forecasting applications", in *Proc. 38th IEEE Photovoltaic Specialists Conf. (PVSC)*, 2012, pp. 1321-1326.

[12] H. D. Gui, Z. Zhang, X. F. He and Y. F. Liu, "A high voltage-gain LLC micro-converter with high efficiency in wide input range for PV applications," in *Proc. IEEE Appl. Power Electron. Conf.*, 2014, pp. 637-642.

[13] S. M. Chen, T. J. Liang, K, H, Chen, M. L. Lao and Y. C. Shen, "A novel switched-coupled-inductor DC-DC step-up converter," in *Proc. IEEE Energy Conversion Congress and Exposition*, 2013, pp. 1830-1833.

[14] S. M. Chen, T. J. Liang, L, S, Yang and J. F. Chen, "A safety enhanced, high step-up DC–DC converter for AC photovoltaic module application," *IEEE Trans. Power Electron.*, vol. 27, no. 4, pp. 1809-1817, Apr. 2012.